

Meson Screening Mass in a Strongly Coupled Pion Superfluid

Yin Jiang, Ke Ren, Tao Xia and Pengfei Zhuang

Physics Department, Tsinghua University, Beijing 100084, China

January 5, 2022

Abstract. We calculate the meson screening mass in a pion superfluid in the framework of Nambu–Jona-Lasinio model. The minimum of the attractive quark potential is always located at the phase boundary of pion superfluid. Different from the temperature and baryon density effect, the potential at finite isospin density can not be efficiently suppressed and the matter is always in a strongly coupled phase due to the Goldstone mode in the pion superfluid.

1 Introduction

Understanding the behavior of quantum chromodynamics (QCD) at finite temperature and density is essential for a description of the development of the early universe and compact stars and for the explanation of the results from high energy nuclear collisions at Relativistic Heavy Ion Collider (RHIC) and Large Hadron Collider (LHC), where high temperature and/or density can be reached. From Lattice simulations [1,2,3,4] at finite temperature, there are two QCD phase transitions, namely the deconfinement transition from hadronic matter to quark matter and the chiral transition from chiral symmetry breaking to its restoration.

At finite baryon density, the QCD phase structure becomes more rich. Besides the deconfinement and chiral phase transitions, the color symmetry which is strict in vacuum is spontaneously broken and leads to a new phase at high density, the so-called color superconductor [5,6,7] which may exist in the core of dense quark stars. However, due to the fermion sign problem [8], there is not yet precise lattice result at finite baryon density. While the properties of the new phases at extremely high density can be studied with perturbative QCD, to investigate the phase transitions themselves at moderate baryon density one needs effective QCD models at low energy.

The isospin symmetry is spontaneously broken when the isospin chemical potential is larger than the pion mass, resulting in the so-called pion superfluid phase [9] which may exist in the core of neutron stars. In comparison with the temperature and baryon density effect, the study on isospin effect or pion superfluid phase includes new phenomena: 1) The isospin structure of QCD phase transitions can be directly examined through lattice simulations without serious technical problems [10,11] emerged at finite baryon density; 2) While for the color superconductivity at finite baryon density the Goldstone modes corresponding to the local color symmetry breaking are eaten up by the Higgs mechanism, the Goldstone mode corresponding to the global isospin symmetry breaking dominates the thermal and dynamic properties of the pion

superfluid [12]; 3) While the phase transitions of deconfinement and chiral symmetry restoration occur at finite temperature and baryon density, there might be no deconfinement [13] and the chiral structure is also significantly changed [14] at finite isospin density.

From the lattice calculated thermodynamics at finite temperature, the energy density [3] and pressure [4] do not reach the corresponding ideal gas limit in the deconfined phase, this means that the quark matter close to the phase transition is not a weakly but a strongly interacting system. The strongly coupled quark matter predicted by the theoretical calculations is recently supported by the strong collective flow [15,16,17] observed in heavy ion collisions at RHIC. It is widely accepted that the coupling strength will decrease with increasing temperature and baryon density, and the quark matter will be in a weakly coupled phase when the temperature or density is high enough.

The potential between two quarks in hot and dense medium can well describe the changes in quark properties at finite temperature and density. It presents a direct way to understand whether the matter is a strongly coupled one. For instance, the heavy quark potential extracted from lattice simulations [18] at finite temperature is the key point to explain the J/ψ suppression [19] observed in heavy ion collisions at RHIC. At finite temperature and baryon density, the effect of chiral symmetry restoration on the quark potential is investigated [20] in the framework of Nambu–Jona-Lasinio (NJL) model [21]. It is found that the minimum of the attractive potential is located at the critical temperature T_c or the baryon chemical potential μ_B^c of the chiral phase transition, and the strongly coupled matter survives only in the temperature region $1 < T/T_c \lesssim 2 - 3$ or baryon density region $1 < \mu_B/\mu_B^c \lesssim 2$. In this paper, we study the meson screening mass and the quark potential at finite isospin density in the NJL model. We will focus on the potential in the pion superfluid and explain its surprising isospin behavior induced by the Goldstone mode corresponding to the spontaneous isospin symmetry breaking.

The original NJL model [21] is inspired by the BCS theory describing normal electron superconductor, and therefore its version at quark level is widely used to describe chiral symmetry restoration, color superconductor and pion superfluid (For reviews and general references, see Ref. [22, 23, 24, 25, 26, 27, 28]). To understand the results of lattice QCD thermodynamics in terms of quasi-particle degrees of freedom, the model is recently extended to include Polyakov loop dynamics (PNJL) [29, 30, 31]. Because of the contact interaction among quarks, there is no confinement in the model and it is necessary to introduce a momentum cut-off Λ to avoid the singularity in momentum integrations. From the uncertainty principle, the minimal length scale in the NJL model is $R \sim 1/\Lambda$. Taking the standard cut-off value $\Lambda \sim 600$ MeV [22, 23, 24, 25, 26], we have $R \sim 1/3$ fm. This means that, the quark potential calculated in the NJL model might be reasonable in the region of $r > 1/3$ fm. In the short range the model is probably not applicable.

The paper is organized as follows. In Section 2 we review the meson propagators in the pion superfluid in the NJL model and calculate the meson screening masses. In Section 3 we calculate the quark potential exactly and in pole approximation, analyze the dominant contribution from the Goldstone mode due to spontaneous isospin symmetry breaking, and discuss the strongly coupled matter in the whole pion superfluid. We summarize in Section 4.

2 meson screening masses

To simplify the numerical calculations, we take the original NJL model and neglect the Polyakov loop potential [29, 30, 31] which disappears at zero temperature. The two flavor NJL model is defined through the Lagrangian density

$$\mathcal{L} = \bar{\psi}(i\gamma^\mu\partial_\mu - m_0 + \mu\gamma_0)\psi + G\left[(\bar{\psi}\psi)^2 + (\bar{\psi}i\gamma_5\tau\psi)^2\right] \quad (1)$$

with scalar and pseudoscalar interactions corresponding to σ and π excitations, where m_0 is the current quark mass, G is the coupling constant with dimension $(\text{GeV})^{-2}$, the quark fields ψ and $\bar{\psi}$, the Pauli operators $\tau = (\tau_1, \tau_2, \tau_3)$ and the quark chemical potential $\mu = \text{diag}(\mu_u, \mu_d) = \text{diag}(\mu_B/3 + \mu_I/2, \mu_B/3 - \mu_I/2)$ are matrices defined in flavor space, and μ_B and μ_I are baryon and isospin chemical potentials. At $\mu_I = 0$, the system has the symmetry $U_B(1) \otimes SU_I(2) \otimes SU_A(2)$, corresponding to baryon number symmetry, isospin symmetry and chiral symmetry. However, the isospin symmetry $SU_I(2)$ is explicitly broken down to $U_I(1)$ global symmetry at small μ_I , and then the $U_I(1)$ symmetry is further spontaneously broken down with condensation of charged pions at large μ_I . At $\mu_B = 0$, the Fermi surfaces of $u(d)$ and anti- $d(u)$ quarks coincide and hence the condensate of u and anti- d quarks is favored at $\mu_I > 0$ and the condensate of d and anti- u quarks is favored at $\mu_I < 0$. A finite μ_B provides a mismatch between the two Fermi surfaces and will reduce the pion condensation.

Introducing the chiral condensate

$$\sigma = \langle \bar{\psi}\psi \rangle \quad (2)$$

and pion condensate

$$\pi = \sqrt{2}\langle \bar{\psi}i\gamma_5\tau_+\psi \rangle = \sqrt{2}\langle \bar{\psi}i\gamma_5\tau_-\psi \rangle \quad (3)$$

with $\tau_\pm = (\tau_1 \pm i\tau_2)/\sqrt{2}$, which are respectively the order parameters for the chiral phase transition and pion superfluid, the inverse of the quark propagator in mean field approximation defined in flavor space

$$\mathcal{S}(p) = \begin{pmatrix} \mathcal{S}_{uu}(p) & \mathcal{S}_{ud}(p) \\ \mathcal{S}_{du}(p) & \mathcal{S}_{dd}(p) \end{pmatrix} \quad (4)$$

can be written as

$$\mathcal{S}^{-1}(p) = \begin{pmatrix} \gamma^\mu p_\mu + \mu_u\gamma_0 - m & 2iG\pi\gamma_5 \\ 2iG\pi\gamma_5 & \gamma^\mu p_\mu + \mu_d\gamma_0 - m \end{pmatrix}, \quad (5)$$

where $m = m_0 - 2G\sigma$ is the dynamic quark mass induced by the spontaneous chiral symmetry breaking. With the quark propagator, the physical condensates σ and π are determined by the gap equations,

$$\begin{aligned} \sigma &= -i \int \frac{d^4p}{(2\pi)^4} \text{Tr} [\mathcal{S}_{uu}(p) + \mathcal{S}_{dd}(p)], \\ \pi &= \int \frac{d^4p}{(2\pi)^4} \text{Tr} [(\mathcal{S}_{ud}(p) + \mathcal{S}_{du}(p))\gamma_5] \end{aligned} \quad (6)$$

with the trace taken in color and Dirac spaces, where the four dimensional momentum integration is defined as $\int d^4p/(2\pi)^4 = iT \int d^3\mathbf{p}/(2\pi)^3 \sum_n$ in the imaginary time formalism of finite temperature field theory with the Matsubara frequency $\omega_n = (2n+1)\pi nT$, $n = 0, \pm 1, \pm 2, \dots$ for fermions.

In the NJL model, the meson modes are regarded as quantum fluctuations above the mean field and can be effectively expressed at quark level in terms of quark bubble summation in random phase approximation (RPA) [22, 23, 24, 25, 26]. In normal phase without pion condensation, the bubble summation selects its specific isospin channel by choosing at each stage the same proper polarization. In the pion superfluid phase, however, the quark propagator contains off-diagonal elements in flavor space, we must consider all possible isospin channels in the bubble summation. In this case, the meson polarization function becomes a matrix in the four dimensional meson space with off diagonal elements [14]

$$\Pi_{jk}(q) = i \int \frac{d^4p}{(2\pi)^4} \text{Tr} \left[\Gamma_j^* \mathcal{S} \left(p + \frac{q}{2} \right) \Gamma_k \mathcal{S} \left(p - \frac{q}{2} \right) \right] \quad (7)$$

with $j, k = \sigma, \pi_+, \pi_-, \pi_0$, where the trace is taken in color, flavor and Dirac spaces, and the meson vertexes are defined as

$$\Gamma_j = \begin{cases} 1 & j = \sigma \\ i\tau_+\gamma_5 & j = \pi_+ \\ i\tau_-\gamma_5 & j = \pi_- \\ i\tau_3\gamma_5 & j = \pi_0 \end{cases}, \quad \Gamma_j^* = \begin{cases} 1 & j = \sigma \\ i\tau_-\gamma_5 & j = \pi_+ \\ i\tau_+\gamma_5 & j = \pi_- \\ i\tau_3\gamma_5 & j = \pi_0 \end{cases} \quad (8)$$

From the definition (7), the polarization function Π is a symmetric matrix in the meson space with $\Pi_{jk} = \Pi_{kj}$, and the neutral pion π_0 is decoupled from the charged

$$\begin{aligned}
\Pi_{\sigma\sigma}(q) &= -3 \int \frac{d^3\mathbf{p}}{(2\pi)^3} \sum_{a,b,c,d=\pm} \left(1 + \frac{m^2 - \mathbf{p}_+ \cdot \mathbf{p}_-}{E_{p_+}^a E_{p_-}^b} \right) \left(v_{p_+}^{ca} u_{p_-}^{db} + u_{p_+}^{(-c)a} v_{p_-}^{(-d)b} \right)^2 \frac{f(\epsilon_{p_+}^{(-c)a}) - f(\epsilon_{p_-}^{(-d)b})}{q_0 + \epsilon_{p_-}^{db} - \epsilon_{p_+}^{ca}}, \\
\Pi_{\sigma\pi_+}(q) &= -3\sqrt{2} \int \frac{d^3\mathbf{p}}{(2\pi)^3} \sum_{a,b,c,d=\pm} \left(\frac{m}{E_{p_+}^a} + \frac{m}{E_{p_-}^b} \right) u_{p_+}^{ca} u_{p_-}^{(-d)b} \left(v_{p_+}^{(-c)a} u_{p_-}^{(-d)b} + u_{p_+}^{ca} v_{p_-}^{db} \right) \frac{f(\epsilon_{p_+}^{(-c)a}) - f(\epsilon_{p_-}^{(-d)b})}{q_0 + \epsilon_{p_-}^{db} - \epsilon_{p_+}^{ca}}, \\
\Pi_{\pi_+\pi_+}(q) &= 6 \int \frac{d^3\mathbf{p}}{(2\pi)^3} \sum_{a,b,c,d=\pm} \left(1 + \frac{m^2 + \mathbf{p}_+ \cdot \mathbf{p}_-}{E_{p_+}^a E_{p_-}^b} \right) \left(u_{p_+}^{ca} u_{p_-}^{(-d)b} \right)^2 \frac{f(\epsilon_{p_+}^{(-c)a}) - f(\epsilon_{p_-}^{(-d)b})}{q_0 + \epsilon_{p_-}^{db} - \epsilon_{p_+}^{ca}}, \\
\Pi_{\pi_+\pi_-}(q) &= -6 \int \frac{d^3\mathbf{p}}{(2\pi)^3} \sum_{a,b,c,d=\pm} \left(1 + \frac{m^2 + \mathbf{p}_+ \cdot \mathbf{p}_-}{E_{p_+}^a E_{p_-}^b} \right) v_{p_+}^{ca} u_{p_+}^{(-c)a} v_{p_-}^{db} u_{p_-}^{(-d)b} \frac{f(\epsilon_{p_+}^{(-c)a}) - f(\epsilon_{p_-}^{(-d)b})}{q_0 + \epsilon_{p_-}^{db} - \epsilon_{p_+}^{ca}}, \\
\Pi_{\pi_0\pi_0}(q) &= -3 \int \frac{d^3\mathbf{p}}{(2\pi)^3} \sum_{a,b,c,d} \left(1 - \frac{m^2 + \mathbf{p}_+ \cdot \mathbf{p}_-}{E_{p_+}^a E_{p_-}^b} \right) \left(v_{p_+}^{ca} u_{p_-}^{db} + u_{p_+}^{(-c)a} v_{p_-}^{(-d)b} \right)^2 \frac{f(\epsilon_{p_+}^{(-c)a}) - f(\epsilon_{p_-}^{(-d)b})}{q_0 + \epsilon_{p_-}^{db} - \epsilon_{p_+}^{ca}} \quad (9)
\end{aligned}$$

pions π_+ and π_- and the isospin singlet σ with $\Pi_{\pi_0\sigma} = \Pi_{\pi_0\pi_+} = \Pi_{\pi_0\pi_-} = 0$. Considering further the relations $\Pi_{\sigma\pi_-}(q) = \Pi_{\sigma\pi_+}(-q)$ and $\Pi_{\pi_+\pi_-}(q) = \Pi_{\pi_+\pi_+}(-q)$, there are only five independent polarization elements $\Pi_{\sigma\sigma}$, $\Pi_{\sigma\pi_+}$, $\Pi_{\pi_+\pi_+}$, $\Pi_{\pi_+\pi_-}$ and $\Pi_{\pi_0\pi_0}$. Taking the trace and performing the fermion frequency summation in (7), and introducing the following definitions based on the quark energy $E_p = \sqrt{\mathbf{p}^2 + m^2}$, $\epsilon_p^{ab} = a\sqrt{(E_p + b\mu_I/2)^2 + 4G^2\pi^2}$, $u_p^{ab} = \sqrt{(1 + (E_p + \mu_I/2)/\epsilon_p^{ab})/2}$, $E_p^a = aE_p$, $v_p^{ab} = au_p^{ab}$ with $a, b = \pm$ and the Fermi-Dirac distribution function $f(x) = 1/(e^{(x-\mu_B/3)/T} + 1)$, the complicated expressions for the polarizations are greatly simplified, and the five independent elements can be explicitly expressed in a compact way in (9), with $\mathbf{p}_\pm = \mathbf{p} \pm \mathbf{q}/2$. Note that there is no Lorentz invariance at finite temperature and density, and the polarization elements are no longer functions of the Lorentz scalar quantity $q^2 = q_0^2 - \mathbf{q}^2$ but depend separately on q_0^2 and \mathbf{q}^2 .

Describing the meson exchange in quark scattering via the quark bubble summation and taking into account the spontaneous isospin symmetry breaking, the meson propagator can effectively be expressed as a matrix in the four dimensional meson space [14]

$$D(q_0^2, \mathbf{q}^2) = \frac{-2G}{1 - 2G\Pi(q_0^2, \mathbf{q}^2)}. \quad (10)$$

The dynamical meson mass M_j in vacuum is defined as the pole of the meson propagator at $q^2 = M_j^2$. At finite temperature and density, the position of the pole is changed to $q_0^2 = M_j^2$, $\mathbf{q}^2 = 0$,

$$\det[1 - 2G\Pi(M_j^2, 0)] = 0, \quad (11)$$

where the symbol \det means the determinant of the matrix $1 - 2G\Pi$. In normal phase without pion condensation, it is simplified to four independent mass equations, $1 - 2G\Pi_{jj}(M_j^2, 0) = 0$. At $\mu_I = 0$ and in chiral limit, it is found [32] that the three pions are the Goldstone modes corresponding to the spontaneous chiral symmetry

breaking and dominate the thermodynamics of the system at low T and low μ_B . In the pion superfluid, however, mesons σ, π_+ and π_- are coupled together and no longer the eigen modes of the Hamiltonian of the system, the new eigen modes, labeled by $\bar{\sigma}, \bar{\pi}_+$ and $\bar{\pi}_-$ are linear combinations of σ, π_+ and π_- . The pole equation (11) in this case is separated into $1 - 2G\Pi_{\pi_0\pi_0}(M_{\pi_0}^2, 0) = 0$ for $\bar{\pi}_0$ (to avoid confusion with the π_0 in normal phase, we still use $\bar{\pi}_0$ to stand for π_0 in the pion superfluid) and $\det[1 - 2G\tilde{\Pi}(M_j^2, 0)] = 0$ for $\bar{\sigma}, \bar{\pi}_+$ and $\bar{\pi}_-$, where the polarization $\tilde{\Pi}$ is the sub-matrix of Π defined in the meson subspace $\{\sigma, \pi_+, \pi_-\}$. The T , μ_B and μ_I dependence of M_j is shown in Ref. [14].

From the Yukawa potential between two nucleons, $V(r) \sim e^{-\mathcal{M}r}/r$, its strength is governed by the mass \mathcal{M} of the exchanged boson. The long range force is suppressed or screened by the massive boson (this is the reason why \mathcal{M} is called the screening mass). Its inverse is the screening length $\mathcal{R} = 1/\mathcal{M}$. At finite temperature, the screening mass is defined as the pole of the boson propagator at $q_0^2 = 0, \mathbf{q}^2 = -\mathcal{M}^2$. In the NJL model at quark level, the meson screening mass \mathcal{M} which control the quark potential are defined as

$$\det[1 - 2G\Pi(0, -\mathcal{M}^2)] = 0, \quad (12)$$

which is again simplified to four independent equations $1 - 2G\Pi_{jj}(0, -\mathcal{M}^2) = 0$ in normal matter for $j = \sigma, \pi_+, \pi_-, \pi_0$ and separated into $1 - 2G\Pi_{\pi_0\pi_0}(0, -\mathcal{M}_{\pi_0}^2) = 0$ for $\bar{\pi}_0$ and $\det[1 - 2G\tilde{\Pi}(0, -\mathcal{M}_j^2)] = 0$ in the meson subspace for $\bar{\sigma}, \bar{\pi}_+$ and $\bar{\pi}_-$ in the pion superfluid.

Before the numerical calculation, we can analytically prove that in the pion superfluid the mass equation (11) at $M = 0$ or (12) at $\mathcal{M} = 0$ becomes exactly the second gap equation of (6) for the pion condensate,

$$\det[1 - 2G\Pi(0, 0)] = 0. \quad (13)$$

This means that the Goldstone mode with $M = \mathcal{M} = 0$, corresponding to the spontaneous isospin symmetry

breaking, is automatically guaranteed in the RPA approximation in the NJL model, and the Yukawa potential via the exchange of the Goldstone meson is not screened.

There are three parameters in the NJL model, the current quark mass m_0 , the coupling constant G and the momentum cutoff Λ . In the following numerical calculations, we take $m_0=5$ MeV, $G=4.93$ GeV $^{-2}$ and $\Lambda=653$ MeV. This group of parameters corresponds to the pion mass $M_\pi=134$ MeV, the pion decay constant $f_\pi=93$ MeV and the effective quark mass $m=310$ MeV in vacuum. To extract reliable conclusions from the numerical calculations in the model, the thermodynamic parameters, namely the temperature and quark chemical potentials, should be much less than the cutoff, $T, \mu_B/3, \mu_I/2 \ll \Lambda$. In our following numerical calculations we take $T < 300$ MeV, $\mu_B < 900$ MeV and $\mu_I < 600$ MeV. Considering the critical isospin chemical potential $\mu_I^c = 134$ MeV [14], $\mu_I = 600$ MeV $\simeq 4\mu_I^c$ is large enough for the discussion of pion superfluid.

With the coupled gap equations (6) for the chiral and pion condensates, the phase boundary of the pion superfluid as a hypersurface in the three dimensional space of temperature and baryon and isospin chemical potentials is shown in Fig. 1. Since the pion condensate increases with decreasing temperature and baryon density and increasing isospin density, the pion superfluid phase is located in the region of low temperature, low baryon density and high isospin density. By comparing the second gap equation of (6) for the pion condensate with the dynamical mass equation (11) for pions, the critical isospin chemical potential for the pion superfluid at $T = \mu_B = 0$ is exactly the pion mass in vacuum, $\mu_I^c = M_\pi = 134$ MeV. This critical value increases with increasing temperature and baryon chemical potential.

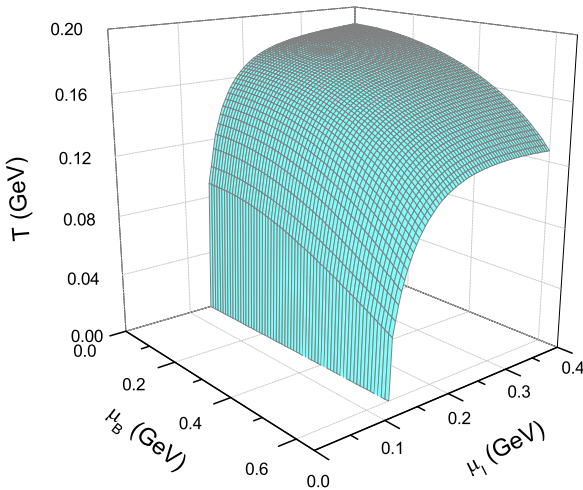


Fig. 1. The phase transition hypersurface of pion superfluid in the three dimensional space of temperature T and baryon and isospin chemical potentials μ_B and μ_I in the NJL model.

The isospin chemical potential dependence of the screening masses at fixed temperature and baryon chemical potential is shown in Fig. 2. For the chosen $T = 100$ MeV

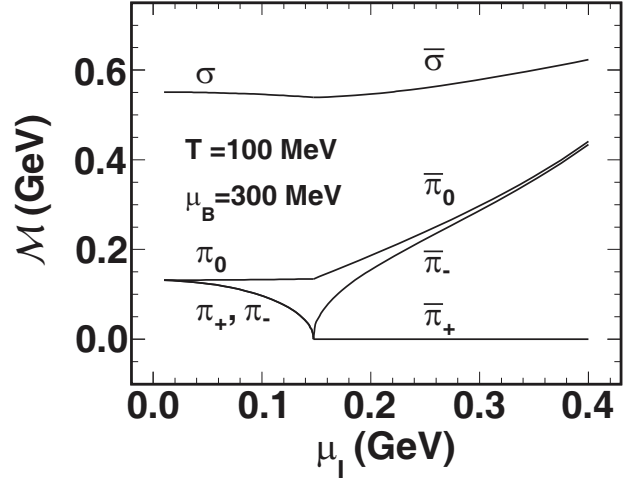


Fig. 2. The meson screening masses \mathcal{M} as functions of isospin chemical potential μ_I at temperature $T = 100$ MeV and baryon chemical potential $\mu_B = 300$ MeV.

and $\mu_B = 300$ MeV, the critical μ_I for the pion superfluid is $\mu_I^c = 142$ MeV. Since mesons carry isospin charge, the isospin dependence of the meson propagator D comes from not only the chiral and pion condensates $\sigma(\mu_I)$ and $\pi(\mu_I)$ but also an explicit shift for the meson energy $q_0 \rightarrow q_0 - \mu_I^j$, $D((q_0 - \mu_I^j)^2, \mathbf{q}^2; \sigma(\mu_I), \pi(\mu_I))$, where μ_I^j is the meson isospin chemical potential. This explicit μ_I dependence leads to a dynamical mass splitting for the charged pions [14] even in the normal phase. For the screening mass defined at $q_0^2 = 0, \mathbf{q}^2 = -\mathcal{M}^2$ of the propagator, however, the explicit and inexplicit isospin dependence in the normal phase is the same for the two charged pions, and therefore they are degenerate in the normal phase. Considering the condensation of π_+ at $\mu_I > \mu_I^c$, \mathcal{M}_{π_+} and \mathcal{M}_{π_-} are different from each other in the pion superfluid. The degeneracy of \mathcal{M}_{π_+} and \mathcal{M}_{π_-} in the normal phase leads to two zero modes at the critical point, which is the reason why the strength of the quark potential approaches to the maximum at the phase transition very fast, see the discussion below. In the pion superfluid, only π_0 is still the eigen mode, but σ, π_+ and π_- are replaced by the new eigen modes $\bar{\sigma}, \bar{\pi}_+$ and $\bar{\pi}_-$. $\bar{\pi}_+$ is the Goldstone mode with zero screening mass $\mathcal{M}_{\bar{\pi}_+} = 0$, as we analyzed above. At small isospin chemical potential $\mu_I < \mu_I^c$, the chiral symmetry $SU_A(2)$ is already explicitly broken to $U_A(1)$. Therefore, the chiral symmetry restoration at high isospin chemical potential means only degeneracy of σ and π_0 , the charged π_+ and π_- behave differently. However, in Fig. 2 the degeneracy at high isospin chemical potential is not for $\bar{\pi}_0$ and $\bar{\sigma}$ but for $\bar{\pi}_0$ and $\bar{\pi}_-$. This is due to the strong mixing among σ, π_+ and π_- [14].

In the top panel of Fig. 3 we show the screening masses in the normal phase as functions of temperature at fixed baryon and isospin chemical potentials $\mu_B = 300$ MeV and $\mu_I = 100$ MeV. The charged pions π_+ and π_- coincide with each other in the whole plane, as we discussed above. Since there is no $\sigma - \pi$ mixing in the normal phase,

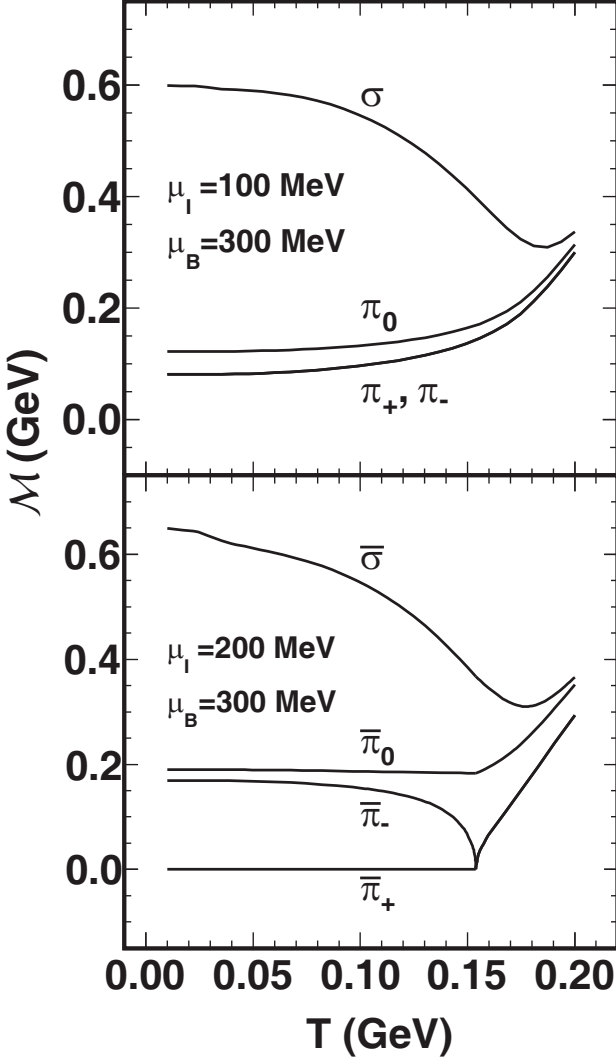


Fig. 3. The meson screening masses \mathcal{M} as functions of temperature T in normal phase (top panel) at isospin chemical potential $\mu_I = 100$ MeV and in pion superfluid (bottom panel) at $\mu_I = 200$ MeV. In both phases the baryon chemical potential is fixed to be $\mu_B = 300$ MeV.

the σ and π_0 mesons become degenerate at high temperature where the chiral symmetry is almost restored. For a small isospin chemical potential, the mass splitting between neutral and charged pions is slight.

In order to clearly see the effect of spontaneous and explicit isospin symmetry breaking on the screening masses, we show in the bottom panel of Fig. 3 their temperature dependence at a higher isospin chemical potential. For the chosen $\mu_I = 200$ MeV and $\mu_B = 300$ MeV, the critical temperature for the phase transition from pion superfluid to normal phase is $T_c \simeq 155$ MeV. In the pion superfluid at $T < T_c$, π_+ is the Goldstone boson with screening mass $\mathcal{M}_{\pi_+} = 0$. Because of the mixing among σ, π_+ and π_-, π_0 and π_- , instead of σ and π_0 , approach to each other at low temperature where the mixing is strong enough. When T is close to the critical point, π_- approaches to the Goldstone mode due to the weakening of the pion

condensation. In normal phase at $T > T_c$, π_+ and π_- coincide again, and with increasing temperature σ and π_0 mesons approach to each other when the chiral symmetry is gradually restored.

3 quark potential

By analogy with the Yukawa potential between two nucleons through one boson exchange, the static quark potential via one meson exchange can be expressed as the Fourier transform of the meson propagator at $q_0 = 0$,

$$V(r) = \int \frac{d^3\mathbf{q}}{(2\pi)^3} D(0, \mathbf{q}^2) e^{i\mathbf{q}\cdot\mathbf{r}}. \quad (14)$$

In the flavor SU(2) NJL model, the meson propagator in the pion superfluid is a 4×4 matrix with off diagonal elements, the quark potential becomes

$$\begin{aligned} V(r) &= \int \frac{d^3\mathbf{q}}{(2\pi)^3} \text{Tr} D(0, \mathbf{q}^2) e^{i\mathbf{q}\cdot\mathbf{r}} \\ &= -\frac{G}{\pi^2 r} \int dq \text{Tr} \frac{q \sin(qr)}{1 - 2G\Pi(0, q^2)}, \end{aligned} \quad (15)$$

where the trace is taken in the meson space $\{\sigma, \pi_+, \pi_-, \pi_0\}$. Note that there is no singularity for the propagator on the real momentum axis and the above integration is numerically straightforward without any technical problem.

To better understand the potential through the screening of the interaction, we take also the pole approximation in calculating the quark potential. In this case the potential can be simplified as a summation over the poles,

$$\begin{aligned} V(r) &= - \int \frac{d^3\mathbf{q}}{(2\pi)^3} \sum_j \frac{g_{jq\bar{q}}^2}{q^2 + \mathcal{M}_j^2} e^{i\mathbf{q}\cdot\mathbf{r}} \\ &= - \sum_j \frac{g_{jq\bar{q}}^2}{4\pi r} e^{-\mathcal{M}_j r} \end{aligned} \quad (16)$$

with $j = \sigma, \pi_+, \pi_-, \pi_0$ in the normal phase and $j = \bar{\sigma}, \bar{\pi}_+, \bar{\pi}_-, \bar{\pi}_0$ in the pion superfluid, where $g_{jq\bar{q}}$ is the effective meson-quark-antiquark coupling constant,

$$g_{jq\bar{q}}^2 = \frac{2G \sum_i \left[\frac{\det[1 - 2G\Pi(0, q^2)]}{1 - 2G\Pi(0, q^2)} \right]_{ii}}{\frac{d}{dq^2} \det[1 - 2G\Pi(0, q^2)]} \Big|_{q^2 = -\mathcal{M}_j^2} \quad (17)$$

which is reduced to

$$g_{jq\bar{q}}^2 = - \left[\frac{d\Pi_{jj}(0, q^2)}{dq^2} \right]_{q^2 = -\mathcal{M}_j^2}^{-1} \quad (18)$$

when the pion condensation disappears.

In the normal phase at zero isospin density, it is easy to expect that the quark potential is gradually weakened by finite temperature and baryon density, and this is confirmed by the lattice simulation [18] and model calculation [20]. What we focus on in this paper is the isospin effect on the

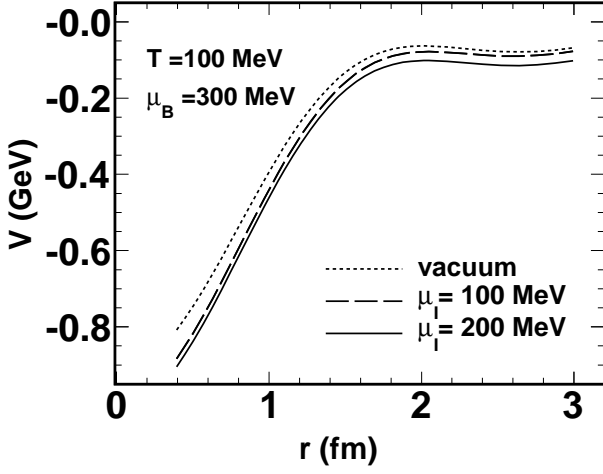


Fig. 4. The quark potential as a function of the distance r between the two quarks in normal phase at $\mu_I = 100$ MeV and in pion superfluid at $\mu_I = 200$ MeV. In both phases the temperature and baryon chemical potential are fixed to be $T = 100$ MeV and $\mu_B = 300$ MeV. The dotted line is the potential in vacuum.

quark potential. In Fig. 4 we show the potential as a function of the distance r between the two quarks in normal phase with $\mu_I = 100$ MeV (dashed line) and in pion superfluid with $\mu_I = 200$ MeV (solid line), the temperature and baryon chemical potential are fixed to be $T = 100$ MeV and $\mu_B = 300$ MeV in the two phases. Considering the momentum cutoff in the model, we do not discuss the potential in short distance and take the starting point $r = 0.4$ fm. The effect of the finite cutoff on the thermodynamics of the system is mainly at high temperature[32]. While this effect is not remarkable in the temperature and density region we considered here, the potential is normalized to $\lim_{T \rightarrow \infty} V(r) = 0$ in the high temperature limit. It is easy to see that this normalization is automatically assumed in the pole approximation (16). In both the normal phase and pion superfluid, the potentials oscillate slightly at large distance. This is from the so called Friedel oscillation [33] induced by the sharp Fermi surface at zero temperature which has been widely discussed in different matters [34, 35, 36]. Since the Fermi surface is smeared at finite temperature, the oscillation is suppressed by temperature and will disappear when the temperature is high enough. The difference between the normal matter and pion superfluid can be understood clearly in the pole approximation (16). From the screening masses shown in Figs. 2 and 3, σ ($\bar{\sigma}$) is always much heavier than the other mesons in the region we discussed, its contribution to the potential is almost screened, and in the intermediate and large distance the potential is mainly from the pion exchange. From Fig. 2, the pion screened masses at $\mu_I = 100$ and 200 MeV satisfy the relations $\mathcal{M}_{\pi_0} < \mathcal{M}_{\bar{\pi}_0}$ and $\mathcal{M}_{\pi_-} < \mathcal{M}_{\bar{\pi}_-}$. If we neglect π_+ and $\bar{\pi}_+$, the potential in the pion superfluid should be above the potential in normal matter. However, when π_+ and $\bar{\pi}_+$ are included, the mass relation $\mathcal{M}_{\pi_+} > \mathcal{M}_{\bar{\pi}_+} = 0$ may turn around the above isospin

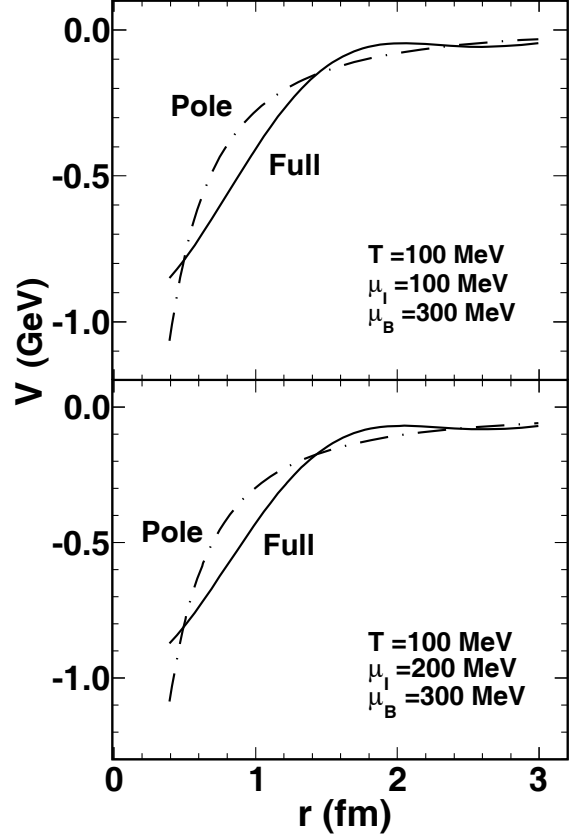


Fig. 5. The quark potential calculated exactly and in pole approximation in normal matter (top panel) with $\mu_I = 100$ MeV and in pion superfluid (bottom panel) with $\mu_I = 200$ MeV. In both phases the temperature and baryon chemical potential are fixed to be $T = 100$ MeV and $\mu_B = 300$ MeV.

dependence, and the attractive potential in the pion superfluid may be stronger than the one in normal matter, namely the potential with $\mu_I = 200$ MeV may be below the potential with $\mu_I = 100$ MeV. This is confirmed from our numerical calculation, as shown in Fig. 4. While for $\mu_I = 100$ and 200 MeV the difference between the two potentials is small, the trend of the isospin dependence is really controlled by the Goldstone mode. We plotted also the potential in vacuum (dotted line) in Fig. 4. Totally different from the temperature and baryon density effect which weakens the interaction among quarks, the potential strength increases with isospin chemical potential.

The above numerical calculation for the potential is full but the analysis on its isospin dependence is based on the behavior of the screening masses. To know to what extent this analysis is valid, we compare in Fig. 5 the exact calculation with the pole approximation in normal matter with $\mu_I = 100$ MeV and in pion superfluid with $\mu_I = 200$ MeV. Again the temperature and baryon chemical potential are fixed to be $T = 100$ MeV and $\mu_B = 300$ MeV in the two phases. While the pole approximation deviates from the full result remarkably in the region of $r < 2$ fm, and the Friedel oscillation is washed away in

the approximation, the screening masses do qualitatively describe the potential, for instance, the exponential decay and the saturation at large distance.

To see clearly and comprehensively the medium effect, we show in Fig. 6 the isospin dependence of the quark potential at a fixed distance. We take $r = 2$ fm which is the typical diameter of a hadron, the potential at this distance can be used to describe the average medium effect on the coupling strength of the quark matter. From the phase diagram Fig. 1, for the chosen baryon chemical potential $\mu_B = 300$ MeV and the isospin region $\mu_I < 600$ MeV, the maximum critical temperature for the pion superfluid is $T_c \simeq 180$ MeV.

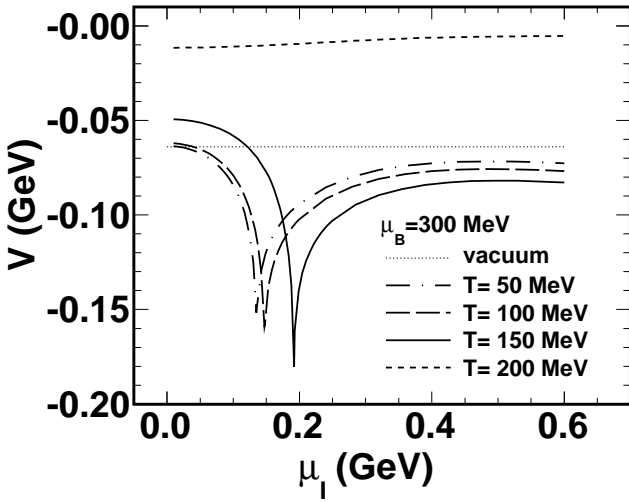


Fig. 6. The quark potential at fixed distance $r = 2$ fm as a function of isospin chemical potential μ_I at fixed baryon chemical potential $\mu_B = 300$ MeV and for different temperature T .

Let us first look at a potential at a given temperature. For any $T < T_c$, the strength of the attractive potential increases with increasing μ_I in normal phase and approaches to the maximum at the critical value μ_I^c . When the system enters the pion superfluid, the behavior of the potential suddenly changes, its strength turns from increasing to decreasing and gets saturated fast. The sharp and deep valley at the critical point μ_I^c arises from the two zero modes π_+ and π_- or $\bar{\pi}_+$ and $\bar{\pi}_-$ at the phase transition, shown in Figs. 2 and 3. Note that the saturated potential in the pion superfluid is always below the vacuum potential $V(r = 2 \text{ fm}) \simeq -0.06$ GeV shown as dotted line in Fig. 6. Therefore, from the valley structure of the potential, the quark matter is most strongly coupled at the phase transition point, and from the strong enough potential at high isospin density, the pion superfluid is always strongly coupled. At $T > T_c$, for instance $T = 200$ MeV, there is no more phase transition, and the valley structure disappears. At such high temperature, the potential at the distance of $r = 2$ fm almost disappears.

We now focus on the temperature dependence of the potential at a given isospin chemical potential, shown in

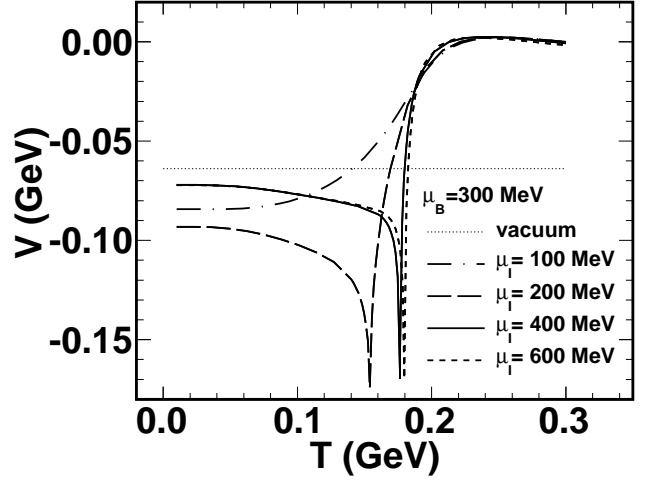


Fig. 7. The quark potential at fixed distance $r = 2$ fm as a function of temperature T at fixed baryon chemical potential $\mu_B = 300$ MeV and for different isospin chemical potential μ_I .

Fig. 7. For a small $\mu_I < 134$ MeV, there is no pion superfluid even at zero temperature, the system is always in the normal phase. In this case, the temperature effect is under our expectation, the potential becomes weaker and weaker in the hot medium and finally vanishes. For a large $\mu_I > 134$ MeV, the system is in pion superfluid at $T < T_c$ and normal phase at $T > T_c$. At a fixed isospin chemical potential, there is also a valley structure around the critical temperature: The potential strength increases with increasing temperature and reaches the maximum at T_c , and after crossing the phase transition point, the potential changes suddenly and turns to become more and more weak and finally disappears. Different from the isospin structure shown in Fig. 6, the potential goes to zero very fast in the normal phase.

4 Conclusion

We have investigated the meson screening masses and quark potential in a pion superfluid in the frame of NJL model. The Goldstone mode corresponding to the spontaneous isospin symmetry breaking plays a significant role in the thermodynamics of the system. The minimum of the attractive quark potential is always located on the phase transition hypersurface in the three dimensional space of temperature and baryon and isospin chemical potentials. While at extremely high temperature and baryon density, quark matter is expected to be in a weakly coupled state, the pion superfluid is in a strongly coupled phase even the isospin density is extremely high. These surprising properties of pion superfluid may help us to understand the isospin asymmetric matter, like the core of compact stars.

In this paper, we considered quarks in mean field approximation and mesons in RPA. When we go beyond the mean field for the pion condensate by taking into account the feedback from the mesons, the phase boundary will be

shifted and the quark potential in the region of low temperature and low densities will be modified, like the case of chiral phase transition [37]. However, the minimum of the potential at the phase transition and the non-zero potential at extremely high isospin density will remain, since they are controlled by the Goldstone mode.

Acknowledgement: The work is supported by the NSFC grant Nos. 10735040, 10847001, 10975084 and 11079024.

References

1. F. Karsch, E. Laermann and A. Peikert, Phys. Lett. **B478** (2000) 447.
2. F. Karsch, Nucl. Phys. **A698** (2002) 199.
3. M. Cheng et al, Phys. Rev. **D81** (2010)054504.
4. S. Borsanyi et al, JHEP, 1011:077 (2010).
5. B. C. Barrois, Nucl. Phys. **B129** (1977) 390.
6. D. Bailin and A. Love, J. Phys. **A12** (1979) L283.
7. D. Bailin and A. Love, Phys. Rept. **107** (1984) 325.
8. S. Muroya, A. Nakamura, C. Nonaka and T. Takaishi, Prog. Theor. Phys. **110** (2003) 615.
9. A. B. Migdal, Zh. Eksp. Teor. Fiz. **61** (1971) 2209.
10. J. B. Kogut and D. K. Sinclair, Phys. Rev. **D66** (2002) 034505.
11. J. B. Kogut and D. K. Sinclair, Phys. Rev. **D70** (2004) 094501.
12. C. Mu and P. Zhuang, Phys. Rev. **D79** (2009) 094006.
13. D. Son and M. Stephanov, Phys. Rev. Lett. **86**, (2001) 592.
14. L. He, M. Jin and P. Zhuang, Phys. Rev. **D71**, (2005) 116001.
15. C. Adler *et al.* [STAR Collaboration], Phys. Rev. Lett. **87** (2001) 182301.
16. J. Adams *et al.* [STAR Collaboration], Phys. Rev. Lett. **92** (2004) 052302.
17. S. S. Adler *et al.* [PHENIX Collaboration], Phys. Rev. Lett. **91** (2003) 182301.
18. O. Kaczmarek and F. Zantow, Phys. Rev. **D71** (2005) 114510.
19. A. Adare *et al.* [PHENIX Collaboration], Phys. Rev. Lett. **98** (2007) 232301.
20. C. Mu and P. Zhuang, Eur. Phys. J. **C58** (2008) 271.
21. Y. Nambu and G. Jona-Lasinio, Phys. Rev. **122**, (1961)345 and **124**, (1961)246.
22. U. Vogl and W. Weise, Prog. Part. and Nucl. Phys. **27**, 195(1991).
23. S. P. Klevansky, Rev. Mod. Phys. **64**, 649(1992).
24. M. K. Volkov, Phys. Part. Nucl. **24**, 35(1993).
25. T. Hatsuda and T. Kunihiro, Phys. Rep. **247**, 221(1994).
26. M. Buballa, Phys. Rept. **407**, 205(2005).
27. D. Ebert and K. G. Klimenko, Phys. Rev. D **80** 125013(2009).
28. D. Ebert and K. G. Klimenko, Eur. Phys. J. C **46** 771(2006).
29. P. N. Meisinger and M. C. Ogilvie, Phys. Lett. **B379** (1996) 163.
30. K. Fukushima, Phys. Lett. **B591** (2004) 277.
31. C. Ratti, M. A. Thaler and W. Weise, Phys. Rev. **D73** (2006) 014019.
32. P. Zhuang, J. Hufner and S. P. Klevansky, Nucl. Phys. **A576** (1994) 525.
33. W. Kohn, Phys. Rev. Lett. **2**, (1959) 393.
34. J. I. Kapusta and T. Toimela, Phys. Rev. **D37** (1988) 3731.
35. J. Diaz Alonso, E. Gallego and A. Perez, Phys. Rev. Lett. **73** (1994) 2536.
36. E. Shuryak, Prog. Part. Nucl. Phys. **62**, (2009) 48.
37. P. Zhuang, Phys. Rev. **C51** (1995) 2256.